


Acquisition of hypoxia inducibility by oxygen sensing N-terminal cysteine oxidase in spermatophytes

Daan A. Weits^{1,2,3} | Lina Zhou^{1,4,5} | Beatrice Giuntoli^{2,6}  | Laura Dalle Carbonare² | Sergio Iacopino^{2,6,7} | Luca Piccinini² | Lara Lombardi⁶ | Vinay Shukla² | Liem T. Bui^{2,8} | Giacomo Novi² | Joost T. van Dongen¹ | Francesco Licausi^{2,6,7} 

¹Institute of Biology 1, Aachen Biology and Biotechnology, RWTH Aachen University, Aachen, Germany

²Institute of Life Sciences, Scuola Superiore Sant'Anna, Pisa, Italy

³Plant-Environment Signaling, Institute of Environmental Biology, Utrecht University, Utrecht, The Netherlands

⁴School of Life Sciences, Lanzhou University, Lanzhou, China

⁵School of Ecology and Environment, Northwestern Polytechnical University, Xi'an, China

⁶Department of Biology, University of Pisa, Pisa, Italy

⁷Department of Plant Sciences, University of Oxford, Oxford, UK

⁸Biotechnology Research and Development Institute, Can Tho University, Can Tho, Vietnam

Correspondence

Francesco Licausi, Department of Plant Sciences, University of Oxford, South Park Rd OX1 3RB Oxford, UK.
Email: francesco.licausi@plants.ox.ac.uk

Daan A. Weits, Plant-Environment Signaling, Institute of Environmental Biology, Utrecht University, Utrecht 3584 CH, The Netherlands.
Email: d.a.weits@uu.nl

Funding information

Ministero dell'Istruzione, dell'Università e della Ricerca, Grant/Award Number: 20173EWRT9; H2020 European Research Council, Grant/Award Number: 101001320

Abstract

N-terminal cysteine oxidases (NCOs) use molecular oxygen to oxidise the amino-terminal cysteine of specific proteins, thereby initiating the proteolytic N-degron pathway. To expand the characterisation of the plant family of NCOs (plant cysteine oxidases [PCOs]), we performed a phylogenetic analysis across different taxa in terms of sequence similarity and transcriptional regulation. Based on this survey, we propose a distinction of PCOs into two main groups. A-type PCOs are conserved across all plant species and are generally unaffected at the messenger RNA level by oxygen availability. Instead, B-type PCOs appeared in spermatophytes to acquire transcriptional regulation in response to hypoxia. The inactivation of two A-type PCOs in *Arabidopsis thaliana*, PCO4 and PCO5, is sufficient to activate the anaerobic response in young seedlings, whereas the additional removal of B-type PCOs leads to a stronger induction of anaerobic genes and impairs plant growth and development. Our results show that both PCO types are required to regulate the anaerobic response in angiosperms. Therefore, while it is possible to distinguish two clades within the PCO family, we conclude that they all contribute to restrain the anaerobic transcriptional programme in normoxic conditions and together generate a molecular switch to toggle the hypoxic response.

KEYWORDS

cysteine oxidation, hypoxia, N-degron pathway, oxygen sensing, plant evolution, regulation of gene expression

This is an open access article under the terms of the Creative Commons Attribution-NonCommercial License, which permits use, distribution and reproduction in any medium, provided the original work is properly cited and is not used for commercial purposes.

© 2022 The Authors. *Plant, Cell & Environment* published by John Wiley & Sons Ltd.

1 | INTRODUCTION

The presence of an electron-rich sulphur sidechain makes cysteine residues extremely reactive and allows for a whole range of oxidative post-translational modifications (Reddie & Carroll, 2008). Some of these states are achieved through the initial oxidation of the free thiol group of cysteine, RSH, to RSOH (cysteine sulfenic acid). The RSOH state is very unstable and therefore can react with a second sulfenic group to generate a disulphide bridge, or RSOH oxidation can proceed to RSO₂H (cysteine sulfinic acid). RSO₂H may be further oxidised to yield the stable RSO₃H state (cysteine sulphonic acid). Therefore, the cysteine oxidation reactions that yield cysteine sulfinic and sulphonic acid are usually considered as irreversible, while cysteine sulfenic acid may be reduced back to cysteine directly or via the formation of a disulphide bridge (Chung et al., 2013). Consequently, cysteine sulfonylation by reactive oxygen species is responsible for changes in selective interaction, enzyme activity and substrate specificity of several proteins.

A specific case is represented by the oxidation of N-terminal cysteinyl residues to sulfinic acid, which has been shown to promote proteasomal degradation in plants and animal cells (Graciet et al., 2010; Hu et al., 2005). The sulfinic group supposedly mimics a carboxyl moiety of the glutamic and aspartic residues, which marks N-terminal degradation signals (N-degrons), following the pathway for proteolysis discovered by Varshavsky and colleagues (Bachmair et al., 1986). Here, the N-terminally exposed oxidised cysteine provides recognition specificity by the N-terminal Arg-transferase (ATE) that catalyzes Arg conjugation. This N-terminal residue, in turn, is recognised by a single subunit E3 ligase Proteolysis 6 (PRT6) that marks the protein for proteasomal degradation with a chain of polyubiquitins (Graciet & Wellmer, 2010; Tasaki et al., 2012). Basal NO levels are also required to maintain the activity of this proteolytic pathway (Gibbs et al., 2014).

In plants and animals, N-terminal sulfonylation of specific proteins is controlled by specific iron-dependent thiol dioxygenases, recently defined as N-terminal cysteine oxidases (NCOs) (Masson et al., 2019; Weits et al., 2014; White et al., 2017). Since these enzymes use oxygen as a co-substrate, the N-degron dependent proteolysis of NCO substrates is promoted under oxic conditions and inhibited by hypoxia (Iacopino and Licausi, 2020). The first plant NCOs, plant cysteine oxidases (PCOs) have been identified in Arabidopsis. Two of them, PCO1 and PCO2, have been initially identified among the proteins that constitute the core low-oxygen response (Weits et al., 2014). The requirement of iron for oxygen coordination in PCOs also generates a response to fluctuations in metal availability (Dalle Carbonare et al., 2019). Only few Arabidopsis proteins with N-terminal cysteine have been confirmed to be substrates of the N-degron pathway: the group VII Ethylene Response Factors (ERF-VIIs), the polycomb group protein Vernalisation 2 (VRN2) and Little Zipper Protein ZPR2 (Gibbs et al., 2011, 2018; Weits et al., 2019). ERF-VIIs are in vivo substrates of

PCO1 and PCO2 (Weits et al., 2014). Oxidation of VRN2 and ZPR2 N-termini by PCO was found to occur at least in vitro, but PCO-dependent degradation still requires confirmation in plants (Taylor-Kearney et al., 2022). All these transcriptional regulators regulate adaptive responses to ambient and internal oxygen fluctuations (Giuntoli et al., 2017; Labandera et al., 2020; Weits et al., 2020). Recently, a metazoans-counterpart of PCO, the Cysteamine Dioxygenase ADO, has also been found to regulate stability of Methionine-Cysteine initiating proteins (Gunawardana et al., 2022; Masson et al., 2019).

The hypoxia-inducible PCOs are not the only members of this small family: for instance in Arabidopsis three additional proteins (namely PCO3, PCO4 and PCO5) share sequence similarity with PCO1 and PCO2. Although all Arabidopsis PCO enzymes have been subjected to biochemical characterisation in vitro (White et al., 2017, 2018), the role of the additional PCOs that are not regulated by ERF-VIIs has not been elucidated in vivo, and the observation that they are not transcriptionally induced upon hypoxia suggests that they may function in different biological processes. In the present study, we characterise two more PCO members with respect to hypoxia responses, PCO4 and PCO5. We focused on these two members starting from the observation that their ablation in *pco1/2* mutant plants caused unprecedented developmental phenotypes, displayed by the quadruple mutant lacking four PCOs (PCO1, 2, 4 and 5). We studied the evolutionary conservation of the non hypoxia-inducible PCOs by performing phylogenetic and functional analyses, and investigated the impact of their genetic inactivation on plant physiology.

2 | METHODS

2.1 | Plant material and growth conditions

Arabidopsis thaliana Columbia-0 (Col-0) was used as wild-type ecotype. Single *pco3* (SALK_017484), *pco4* (GABI_740F11) and *pco5* (SALK_128432) knockout seeds were obtained from the Nottingham Arabidopsis Stock Centre (NASC). The *pco1/2* line (*pco1*: GK-534D06, *pco2*: SM_3.29843) and the quadruple mutant *pco1/2/4/5* (*4pco*) were described previously (Masson et al., 2019; Weits et al., 2014). Homozygous lines were identified via PCR screening of genomic DNA using gene-specific primers together with transfer DNA (T-DNA)-specific primers, as specified in the aforementioned papers. Double homozygous lines were obtained by crossing the two single mutants and then screening the F2 generation as described above. *Pinus pinea* nuts were collected along the Arno river in a 300 m² area centred around Google maps coordinates 43.704733, 10.424682. *Pteris vittata* spores were collected from spontaneous plants found in the garden surrounding Casa Pacini of the Department of Crop Plants of the University of Pisa (coordinates 43.711955, 10.412215). *Selaginella moellendorffii* was purchased from Bowden Hostas (www.bowdenhostas.com) and

propagated asexually. *Physcomitrella patens* was provided by Tomas Morosinotto (University of Padova). *Marchantia polymorpha* Cam2 was provided by Linda Silvestri (University of Cambridge).

Growth in soil of *Arabidopsis* plants: seeds were sown in moistened soil containing peat and perlite in a 3:1 ratio, stratified at 4°C in the dark for 48 h and then germinated at 22°C day/18°C night with a photoperiod of 8 h light and 16 h darkness with 80–120 $\mu\text{mol photons m}^{-2} \text{s}^{-1}$ intensity. For qPCR experiments on adult plants, 5-week-old plants were treated with low-oxygen in plexiglas boxes flushed with a humidified artificial atmosphere containing nitrogen and oxygen in the proportions defined in the results section.

Axenic growth of *Arabidopsis* plants: seeds were sterilised using 70% ethanol for 1 min, incubated in 0.4% sodium hypochlorite (NaClO) for 10 min, rinsed six times with 1 ml distilled sterile water and finally resuspended in 1 ml sterile water. Growth in liquid medium was performed inoculating 100 μl of seed suspension, corresponding to 20–40 seeds, in 2 ml of sterile half-strength MS medium (basal salt mixture 2.15 g L^{-1} , pH 5.7) supplemented with 1% sucrose in each well of 6-well plates. Seeds were incubated in the dark at 4°C for 48 h and subsequently germinated for 4 days at 22°C day/18°C night with a photoperiod of 12 h light and 12 h darkness. Growth on solid medium was performed in square dishes (10 cm side) containing 40 ml of solid MS half-strength medium supplemented with 1% sucrose and 0.8% agar. After stratification for 48 h at 4°C in the dark, germination and growth of the plants occurred at 22°C day/18°C night with a photoperiod of 12 h light and 12 h darkness. Plates were maintained in horizontal or vertical position as described in figure legends.

Pinus pinea, *Pteris vittata* and *Selaginella moellendorffii* were grown on perlite soil under growth chamber conditions as described above for *Arabidopsis thaliana*. Plantlets of *Populus alba* 'Villafranca' clone were maintained in in vitro conditions and treated with hypoxia as described in Dalle Carbonare et al. (2019). *Physcomitrella patens* was cultured in sterile conditions on solid Knop medium as described in (Reski & Abel, 1985) while *Marchantia polymorpha* in solid MS half-strength medium (0.9% wt/vol agar).

2.2 | Low oxygen treatments

Plants were subjected to low oxygen treatments inside plexiglas boxes continuously flushed with an artificial humidified atmosphere containing a mixture of oxygen and nitrogen gases, according to the ratios defined in the results section. During the hypoxic treatments, the boxes were maintained in the dark to avoid oxygen release by photosynthesis. Individual boxes were used for each time point to avoid cycles of hypoxia and reoxygenation. Plants used for control samples were maintained in the dark for an equal amount of time. Survival rates were calculated based on emergence of new leaves on treated

individuals, scored 7 days after the exposure to anoxic conditions. Submergence was imposed to 4-week-old plants grown in soil as described above, inside tanks in a dark climate controlled room. Deionized water was equilibrated for 12 h to the room temperature before pouring it slowly into the tanks up to 15 cm above the plants.

2.3 | Cloning of the plant and bacterial expression vectors

Coding sequences and promoters were amplified from complementary complementary DNA (cDNA) or genomic DNA templates respectively using the Phusion High Fidelity DNA-polymerase (New England Biolabs). RAP2.12_{1–28}-LUC and ZPR2-LUC gene fusions were obtained by overlapping PCR. All open reading frames were cloned into pENTR/D-TOPO (Thermo Fisher Scientific). A DNA fragment coding for mClover3-RAP2.3_{2–70}-mRuby was synthesised by GeneArt (Thermo Fisher Scientific) with attB1 and attB2 adapters (sequence in File S1). The resulting entry vectors were recombined into destination vectors using the LR reaction mix II (Thermo Fisher Scientific) to obtain the novel expression vectors. A complete list and description of the destination vectors and oligonucleotides used in this study is provided in Tables S1 and S2, respectively.

2.4 | Sequence similarity searches

Identification of NCO protein sequences in different sequenced plant species was performed by searching the Phytozome database (www.phytozome.net). *Pteris vittata* and *Pinus pinaster* sequences (the most closely related species to *Pinus pinea* available) were retrieved from the 1000 Plants transcriptome database (www.onekp.com) and EuropineDB (<http://www.scbi.uma.es/pindb/>), respectively. Fungal sequences were obtained from the MycoCosm portal (Grigoriev et al., 2014) (<https://mycocosm.jgi.doe.gov/mycocosm/home>). Protein sequences similar to *Arabidopsis thaliana* PCO1 and PCO4 were retrieved using the BLAST algorithm (Altschul et al., 1990). The sequences obtained in this way were subsequently aligned back against the *Arabidopsis thaliana* protein database to ensure that they represent the closest homologs of AtPCOs.

2.5 | Promoter analyses

A total of 1 kb-long genomic sequences upstream of each PCO gene translation start position (ATG) were downloaded from the Phytozome (<https://phytozome.jgi.doe.gov/pz/portal.html>) or Ensembl (<https://www.ensembl.org/index.html>) portals. Whenever annotated, the 5'-untranslated region (UTR) region was also included in the analysis. The presence of hypoxia responsive

promoter element (HRPE) (Gasch et al., 2016) cis-regulatory sequences was assessed using the FIMO package of MEME-suite 5.1.1 (Bailey et al., 2009). For each promoter, the number and position of HRPE elements was retrieved and noted in Table S3 and File S2, respectively.

2.6 | Phylogenetic analysis

Phylogenetic analysis was performed using MEGAX (Kumar et al., 2018), by applying the Maximum Likelihood method and a JTT matrix-based model (Jones et al., 1992). To generate the phylogenetic tree, NCO protein sequences from different species were aligned using the MUSCLE algorithm (Edgar, 2004) and the initial trees were obtained by applying Neighbour-Join and BioNJ algorithms. The tree with the highest log-likelihood was selected and the bootstrap analysis (500 repeats) returned the percentage of trees in which the associated taxa clustered together.

2.7 | Assessment of gene expression levels

Total RNA extraction, DNase treatment, cDNA synthesis and RT-qPCR analysis was performed as described previously (Kosmacz et al., 2015). RT-qPCR primer sequences are provided in Table S2.

2.8 | Plant transformation

Stable transgenic plants expressing the *PCO4prom:GUS* construct specified in Tables S1 was obtained using the floral dip method (Clough & Bent, 1998). T0 seeds were screened for kanamycin resistance to identify independent transgenic plants. T3 generation plants were used for the experiments. Transient gene expression in *Nicotiana benthamiana* with *35S:GFP-PCO1-5* was performed as described previously (Panucci et al., 2020).

2.9 | Protoplast isolation

Arabidopsis leaf mesophyll protoplasts were produced as described in detail in Iacopino et al. (2019). Leaves from 4-week-old plants were used as starting material for protoplast isolation.

2.10 | Confocal imaging

For GFP-PCO imaging, the abaxial side of leaves from transiently transfected *Nicotiana benthamiana* (4 weeks old) were analysed with a Leica DM6000B/SP8 confocal microscope (Leica Microsystems) using 488-nm laser light (20% laser transmissivity), photomultiplier tube detection, and emission light was collected between 491 and

551 nm. Images were analysed and exported using the LAS X life science software (www.leica-microsystems.com), with an unchanged lookup table settings for each channel. Imaging of the ratiometric mClover3-Ubi-RAP2.3₂₋₇₀-mRuby reporter was performed using a Zeiss airyscan 800. Fiji was used to quantify mClover3 and mRuby mean fluorescence intensity in protoplast nuclei.

2.11 | Luciferase transactivation assay

Transactivation assays were performed using a dual luciferase assay based on *Renilla reniformis* and *Photinus pyralis* luciferase enzymes. A 31 nt long sequence containing the HRPE element was used from the LBD41 promoter (−364 to −331 from the initial ATG), repeated five times in tandem and fused to a minimal 35S promoter, as previously described (Weits et al., 2019). This sequence was synthesised by Geneart (Thermo Fisher Scientific), inserted into pENTR/D-topo (Thermo Fisher Scientific) and recombined into the *pGREEN800LUC* plasmid (Hellens et al., 2005) using LR clonase mix II (Thermo Fisher Scientific) to generate the reporter vector 5xHRPE:PPLuc. To evaluate the effect of PCO proteins on RAP2.12-mediated activation of the 5xHRPE promoter, the effector plasmids were produced by recombining the CDS of PCOs, GFP and RAP2.12 from pENTR-D/TOPO into p2GW7 (Karimi et al., 2002). Mesophyll protoplasts were prepared as indicated above and transfected with three micrograms of each plasmid. Proteins were extracted from protoplasts after a 16 h incubation in WI medium using 100 µl of 1 × passive lysis buffer (Promega). Luciferase activities were measured using the Dual Luciferase Reporter Assay kit (Promega) with a Glomax 20/20 (Promega).

2.12 | Quantification of ethanol production

One week-old *Arabidopsis* seedlings were peeled from vertical plates and incubated for 12 h in 6-well plates (Corning) in 1 ml of liquid half-strength MS medium (pH 5.8) supplemented with 2% sucrose (wt/vol) with shaking. At the end of the light phase of the day, seedlings were treated in plexiglas boxes with normoxia or anoxia (<0.01% O₂ vol/vol) for 12 h. At the end of the treatment, the medium was collected and the ethanol release per milligram of fresh weight of plant material was measured as described by Licausi et al. (2010).

3 | RESULTS

3.1 | Protein sequence and transcriptional regulation distinguish two conserved PCO clades

Whereas *PCO1* and *PCO2* are considered as part of the core anaerobic response genes in *Arabidopsis* (Mustroph et al., 2009), the transcriptional inducibility of the other three members has not been studied in detail. We therefore tested their messenger RNA (mRNA)

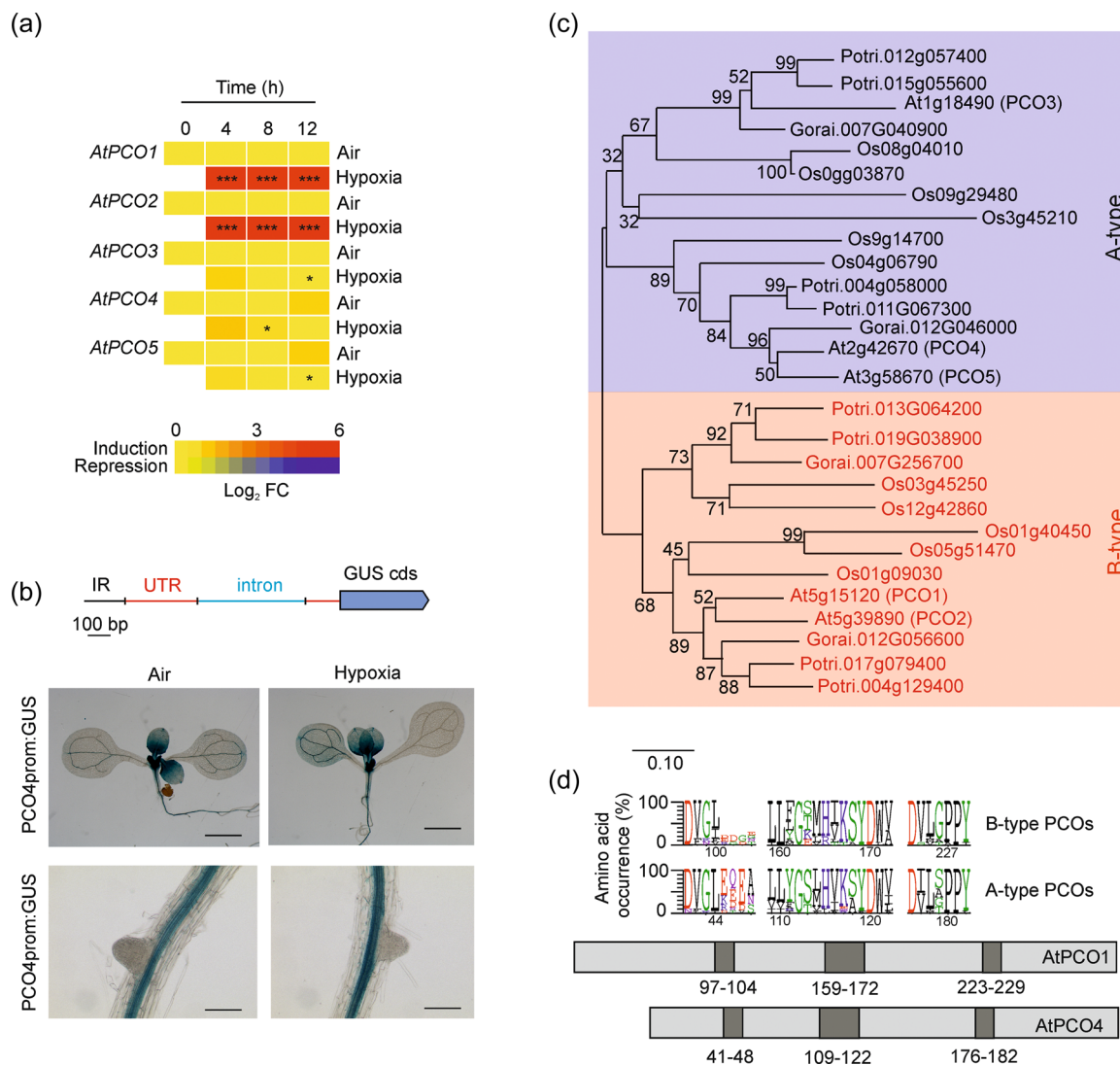


FIGURE 1 Hypoxic regulation of PCO genes in angiosperm species. (a) Expression analysis of the five PCO genes present in the Arabidopsis genome in response to hypoxia. mRNA was extracted from 4-day-old seedlings grown in liquid medium treated for 0, 4, 8 and 12 h of hypoxia in the dark (1% O₂ vol/vol) and the expression of PCOs was compared to that of plants kept under normoxic conditions in the dark. Asterisks indicate statistically significant difference after one-way ANOVA and Tukey's post hoc test (*, 0.01 < *p* < 0.05, ***, *p* < 0.001; *n* = 4). Numeric expression values are shown in Table S4. (b) Visualisation of PCO4 promoter activity by GUS-reporter staining in 7-day-old seedlings, grown in vertical MS-agar plates, treated with 6 h normoxia or hypoxia (1% O₂ vol/vol). (c) Phylogenetic tree illustrating the relatedness of PCO proteins encoded by angiosperms for which transcript data about low oxygen responses are available: *Arabidopsis thaliana* (*At*), *Populus trichocarpa* (*Potri*), *Oryza sativa* (*Os*), and *Gossypium raimondii* (*Gorai*). The genes that encode for the PCOs that were shown to be significantly upregulated upon low oxygen exposure are indicated in red (*p* < 0.05). The Maximum likelihood method and JTT matrix-based model was used to generate an unrooted tree of PCOs. Branch lengths represent the number of substitutions per site. The percentage of trees in which the associated isoforms clustered together is shown next to the branches. Protein sequences used for the alignment are listed in Table S5 along with their respective gene expression data. The multialignment used to generate the phylogenetic tree is displayed in File S3. (d) Amino acid occurrence in the three conserved regions that show the largest variation between A-type and B-type PCO clades. Their position in AtPCO1 (a representative B-type member) and AtPCO4 protein (a representative A-type member) is shown at the bottom of the panel. Letter heights represent percentage of occurrence. ANOVA, analysis of variance; mRNA, messenger RNA

level in response to low oxygen conditions (1% O₂ vol/vol) in a time course over 12 h, corresponding to the light phase of the day. We confirmed that PCO1 and PCO2 are low-oxygen responsive, whereas no clear pattern of induction could be observed for the other three PCO genes (Figure 1a, Table S4, Figures S1–S3). However, previous analysis of microarray data showed that also PCO4 is moderately

induced during late hypoxia treatments (Weits et al., 2014). Therefore, to further verify whether hypoxic regulation is imposed at the transcriptional level, we generated the PCO4prom:GUS reporter line where the 1271-nt long upstream genomic region of the PCO4 gene, including the intergenic sequence before the start of transcription and the 5'-UTR, was fused to the first 24 nt of the

PCO4 coding sequence followed by the beta-glucuronidase (*GUS*) gene (Figure 1b). In 7-day-old seedlings grown under aerobic conditions, *GUS* activity was observed in the vasculature, leaf primordia and basal zone of the first true leaves (Figure 1b). No increase in *GUS* staining was observed after exposure to 6 h hypoxia in the dark, in either shoot or root tissues (Figure 1b). We, therefore, concluded that *PCO4*, similar to *PCO3* and *PCO5* is not induced by low oxygen conditions.

To examine the phylogenetic relationships between low oxygen-responsive and -insensitive PCOs, we retrieved PCO-like sequences from angiosperm species for which the transcriptional response to low oxygen has been characterised at the whole-genome level: *Arabidopsis*, rice (*Oryza sativa*), poplar (*Populus trichocarpa*), cotton (*Gossypium hirsutum*) (Table S5). Since not all poplar sequences were represented on the microarray analysis available, we compared their expression level between aerobic and hypoxic (4 h 1% O₂ vol/vol) conditions in a local poplar accession (*P. alba* 'Villafranca' clone). We aligned these putative orthologous amino-acid sequences and built a phylogenetic tree based on the conserved regions shared among them. The whole set of sequences separated clearly into two main clades: one (A-type PCOs) with proteins whose respective mRNA levels were not upregulated under low oxygen conditions, and a second clade (B-type PCOs) containing all low-oxygen inducible sequences (Figure 1c, Tables S3 and S5). The two clades could be distinguished primarily due to the presence or identity of three different conserved regions found within the ADO/PCO domain (Interpro id IPR012864): a Glu/Asp acid triad at the beginning of the conserved domain (position 45–47 in AtPCO4), which is absent in the hypoxia-inducible PCOs; a substitution of Tyr with Phe/Leu towards the centre of the B-type ADO/PCO domain (position 161 in AtPCO1); and the fixation of a Gly residue instead of an Ala/Thr within the highly conserved C-terminal part (Figure 1d). This result hinted at a concomitant conservation of structural and cis-regulatory features for PCO genes in angiosperms.

3.2 | The HRPE is conserved in the promoter of inducible PCO genes

The inducibility of B-type PCO genes by low oxygen conditions in the angiosperm species considered before is likely explained by the transcriptional regulation imposed by RAP2-type transcription factors, since this has been demonstrated in *Arabidopsis* previously (Gasch et al., 2016). Indeed, when analyzing 1 Kb of the 5' genomic sequence preceding the ATG start codon of each hypoxia-inducible PCO-coding gene, we found 1–4 repeats of the HRPE, identified as the main DNA feature recognised by the ERF-VII transcription factors (File S2 and Table S3). This 9 bp-long motif occurred both in the 5'-UTR and the upstream intergenic region. Only in the case of the *Loc_Os1g09030* gene, the HRPE element was found inside a long 5'-UTR, 1270 bp upstream of the initial ATG codon (File S2 and Table S3). We could only identify the same motif in the genomic region upstream of a subset of the A-type PCO genes (25/115),

mostly present in a single repetition (Table S3). A Chi-square analysis confirmed a significant correlation ($p \leq 0.001$) between the occurrence of at least one HRPE element in the promoter or 5'-UTR and the regulation imposed by hypoxia. These results support the hypothesis that genes coding for B-type PCOs are controlled by ERF-VII transcription factors. Analysis of the GCC-box motif, also identified as potential ERF-VII binding site (Gasch et al., 2016; Gibbs et al., 2014), in the 5'-UTR and 1 kb promoter sequences of PCO genes revealed its occurrence in some sequences of both A-type and B-type PCOs. However, we found no significant correlation between the presence of the GCC motif and hypoxia-inducibility of the corresponding PCO gene (File S2 and Table S3).

3.3 | Hypoxia-inducible B-type PCOs have been acquired and conserved in spermatophytes

The identification of two separate clades of PCOs led us to question when this separation occurred during plant evolution, with possible implications in the mechanisms of oxygen perception in photosynthetic eukaryotes. We therefore searched for PCO-like sequences in genomes and transcriptomes of species belonging to taxa that could represent stepwise acquisition of traits that belong to actual angiosperms. To the angiosperm sequences used for the analysis shown in Figure 1c before, we added those of *Pinus pinea* and *Picea abies* for gymnosperms, *Pteris vittata* and *Botrypus virginianus* for pteridophytes, *Selaginella moellendorffii* and *Lycopodium annotinum* for lycophytes, *Physcomitrella patens* and *Marchantia polymorpha* for bryophytes. We also included three members of the green algae taxon: *Volvox carteri*, *Chlamydomonas reinhardtii* and *Dunaliella salina*. Reciprocal Blast-search using *Arabidopsis* PCOs as a reference showed that B-type sequences are present in tracheophytes including pteridophytes and spermatophytes, although only consistently found ubiquitous in the latter. On the other hand, bryophyte species only contained A-type proteins (Table S3).

We expanded this initial analysis, by taking into consideration 212 PCO-like sequences from 42 plant species whose genome has been fully sequenced, including two belonging to the rodophyta and one from the glaucophyta taxa (Figure 2 and Table S3). All sequences identified contain an ADO/PCO domain, characterised by highly conserved His residues in position 98, 100 (with respect to the PCO4 sequence) and, to a lesser extent, 164, which are involved in metal coordination and which are essential for dioxygenation catalysis (McCoy et al., 2006). Based on the three structural features identified above and depicted in Figure 1d, all PCO sequences from embryophytes could be distinguished in A- and B-types. In few cases, ambiguous attribution to either one of the two clades was solved by reciprocal blast against the *Arabidopsis* proteome. Algae PCO instead showed characteristics of both clades and were therefore considered as a separate uncertain category (Figure 2 and Table S3). The highest number of PCO-coding genes was observed in monocots, fabales and *Malus domestica* among the

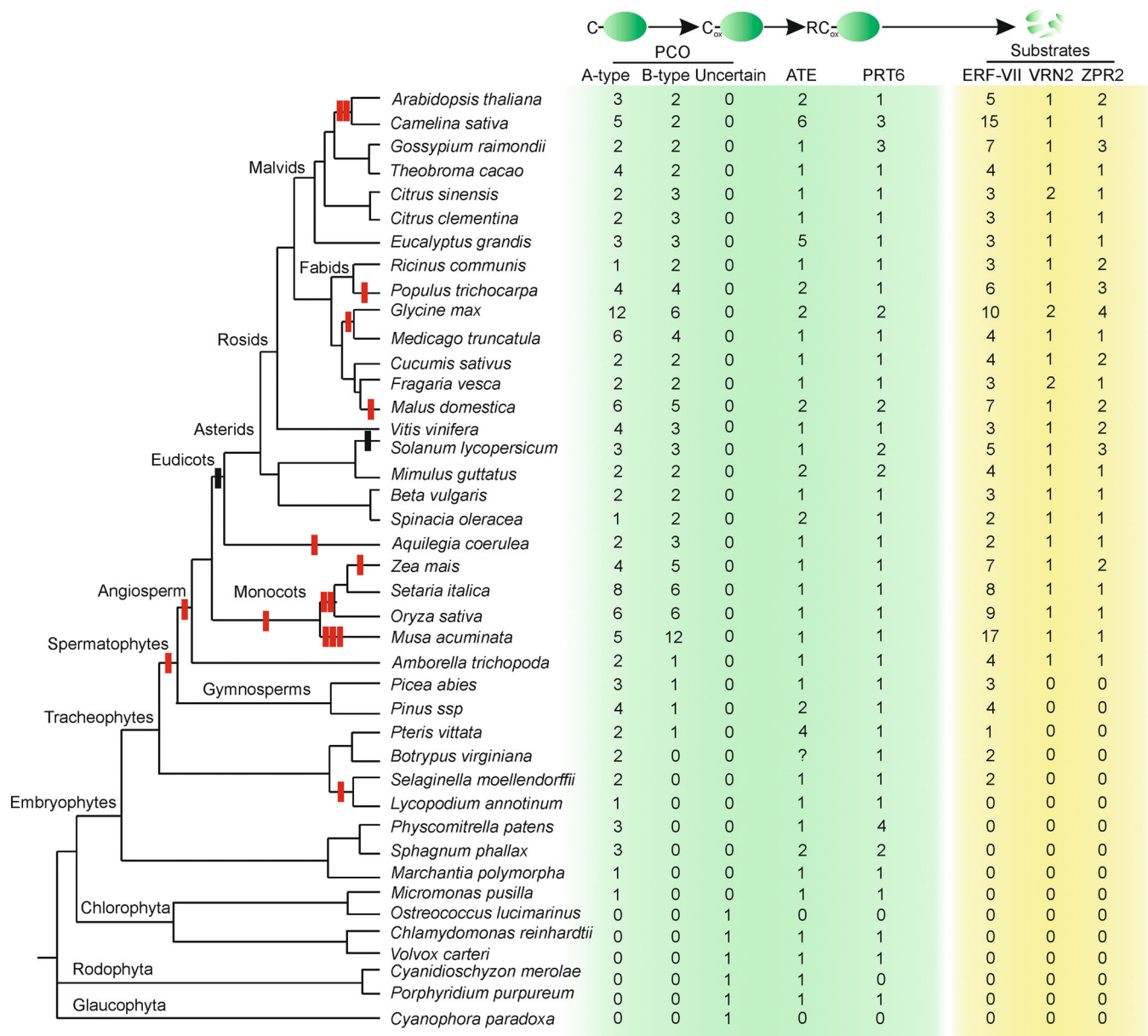


FIGURE 2 Evolutionary conservation across plant species of components of the oxygen-dependent branch of the N-degron pathway and their known targets. Whole-genome duplications are shown with vertical red bars for the branches corresponding to land plants, as described in Liu et al. (2016). Vertical red ticks indicate genome duplication event, vertical black ticks represent genome triplication events. The number of non-identical sequences attributed to each class of predicted proteins and clade assignment for each PCO sequence is shown on the right side of the tree. ATE and PRT6 sequences in *Pinus spp* were retrieved from the *Pinus taeda* predicted proteome, while PCO and ERF-VII sequences have been confirmed by cloning and sequencing from *Pinus pinea* messenger RNA. Question marks indicate partial correspondence (identification of sequences that correspond to portions of the protein used as the bait). [Color figure can be viewed at wileyonlinelibrary.com]

rosales class, in agreement with the progression in genome size due to duplication events (Liu et al., 2016). Although the ratio of B-type to A-type PCO varies considerably between species, at least one representative of both clades could be found in all spermatophytes considered. Among ferns and lycophytes, instead, only A-type PCOs were found, except for *Pteris vittata* which appeared to also contain a B-type PCO protein (Figure 2 and Table S3).

Finally, we interrogated public sequence databases to evaluate the co-occurrence of PCOs with the other two enzymes that act in

the Arg/N-degron pathway, ATE and PRT6, and established the evolution of Cys N-degron substrates in the green lineage. We confirmed ubiquitous ATE and PRT6 presence in each examined species, although we could not always detect homologs in red algae, glaucophytes and green algae (Figure 2). Cys-initiating proteins belonging to the ERF-VII group were identified in spermatophytes, including lycophytes (Figure 2 and Table S3), as previously indicated (Holdsworth and Gibbs, 2020). VRN2 and ZPR2 confirmed instead to have undergone later fixation of their Cys-initiating identity, in

angiosperms (Figure 2 and Table S3; Gibbs et al., 2018; Weits et al., 2020).

We therefore speculated that the A-type PCOs represent the earliest form of plant NCO, which acquired the ability to regulate the stability of a specific ERF group in vascular plants. Moreover, in spermatophytes the B-group PCO diverged from the original clade and acquired, at the gene level, ERF-VII-dependent inducibility through the HRPE motif.

3.4 | Chytrids are the only fungal species with PCO-like proteins

Since the existence of N-terminal cysteinyl-dioxygenases (NCOs) has been confirmed in both plants and animals (Holdsworth and Gibbs 2020; Masson et al., 2019; Weits et al., 2014), we investigated their

occurrence in the fungal kingdom. A thorough search throughout the proteome of fungi species whose genome has been fully sequenced returned hits only within the chytrid clade (Figure 3a), although not all chytrid species tested showed a PCO-like sequence (Table S6 and Figure S4). Reciprocal identification of ADOs or PCOs in plant and metazoan databases using these fungal sequences as baits confirmed the orthology of the sequences. The presence of PCO/ADO-like sequences in almost all chytrid species in the database, but not in other phyla, can be interpreted as the loss of this enzymatic function in the fungal kingdom, while it was retained in chytrids. Alternatively, one can speculate about the acquisition of this enzyme exclusively by this latter fungal clade from a plant or metazoan host. We thus compared the most conserved regions identified in the ADO/PCO domain of species from the main phyla of the three kingdoms and used the resulting alignment to generate a phylogenetic tree with the Maximum Likelihood algorithm (Figure 3b,c). Grouping of proteins

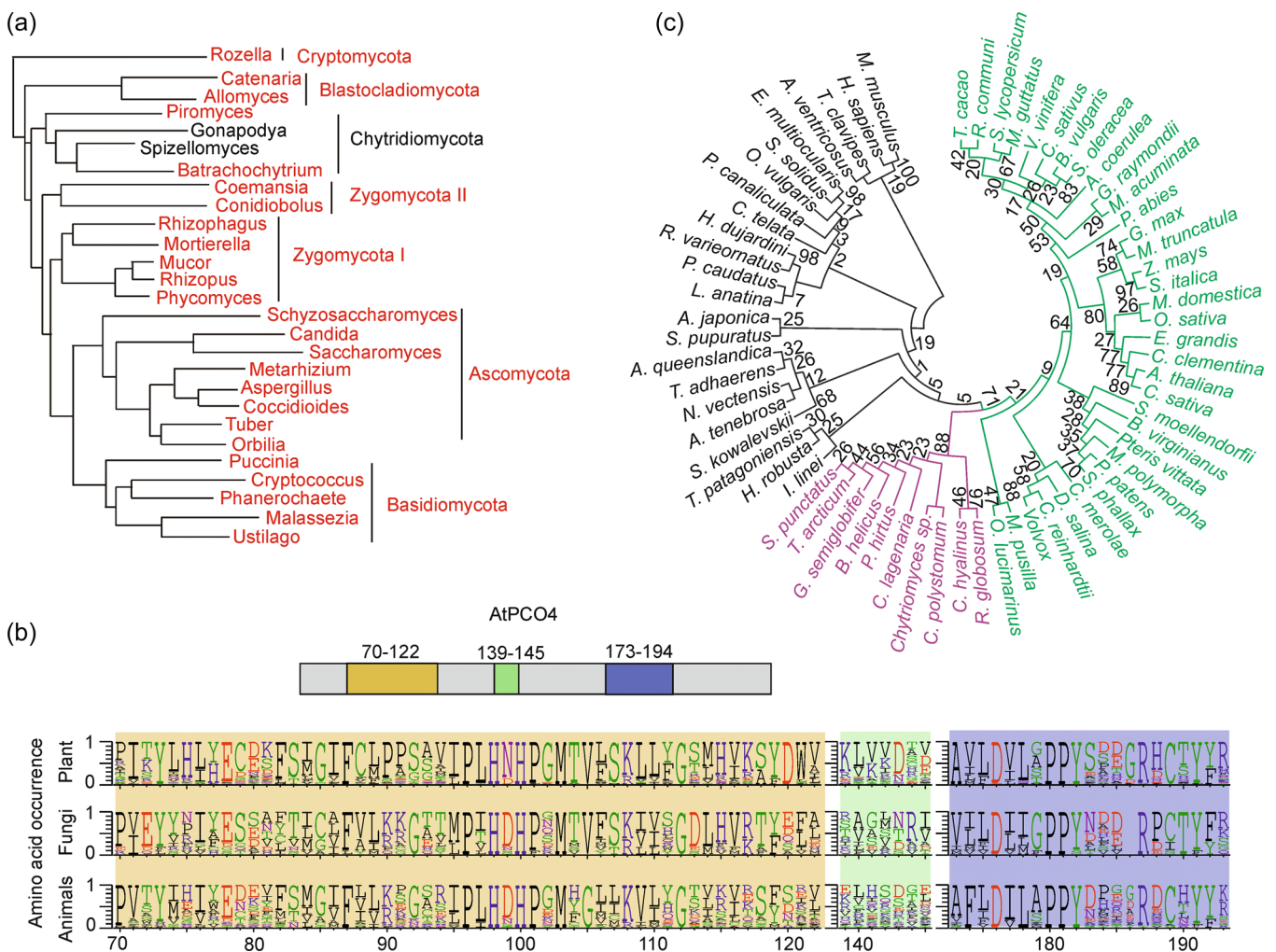


FIGURE 3 Presence of NCO-like sequences across the fungal kingdom. (a) The phylogeny of fungi is based on the analysis by Chang et al. (2015). Species whose genome does not contain any NCO-like coding gene are marked in red. (b) Amino acid occurrence in three conserved regions of NCOs in animals, plants and fungi. Their position in AtPCO4 protein is shown at the top of the panel. (c) Relatedness of NCO proteins across the three eukaryotic kingdoms (plants in green, fungi in purple and animals in black), inferred by using the Maximum Likelihood method and JTT matrix-based model. Results of the bootstrap analysis are shown next to each branch. NCO, N-terminal cysteine oxidases [Color figure can be viewed at wileyonlinelibrary.com]

reflected the assignment of original species into the three kingdoms, with chytrid putative NCOs clustering closer to plant PCOs than to metazoan ADOs (Figure 3b,c). In light of this result, since the speciation of Viridiplantae is estimated to have occurred before the separation of animals from fungi, we favoured the hypothesis of horizontal transfer of PCO-like gene from an ancestral green organism to a chytrid progenitor.

3.5 | B-type PCO conservation is extended to the transcriptional regulation

Next, we investigated whether the genes encoding for B-type PCOs share conserved regulation by hypoxic conditions. Therefore, we quantified the mRNA levels of the PCO genes in one species of each taxon considered to generate the signature motifs depicted in Figure 1d, selected depending on plant material available on site. Relative expression levels were monitored by real-time RT-qPCR, comparing mRNA extracted from samples exposed for different duration of hypoxic stress (1% O₂ vol/vol). Control samples were maintained in the dark and harvested at the same time of the day, to disambiguate between possible circadian regulation and true hypoxic induction. Moderate transcriptional upregulation by hypoxia was recorded for the only B-type gene found in this set of species, PCO5 of *P. pinea*. High response was instead observed for pine PCO1, which shared the strongest sequence similarity to the non hypoxia-inducible A-type PCOs of angiosperms (Figure 4 and Table S7). Among more early diverging species, mild upregulation was observed for *P. vittata* PCO2 and *P. patens* PCO2, although mRNA of *P. patens* followed a similar trend under aerobic conditions in darkness (Figure 4). PCO-like genes belonging to *S. moellendorffii* and *M. polymorpha* did not show altered expression in response to hypoxia. A search for HRPE-like elements in the 5'upstream region of the *P. patens* PCO2 gene did not lead to any positive identification (File S2), suggesting that its transcriptional regulation likely occurs via a different class of transcription factors or following an alternative mechanism.

In conclusion, our results showed that early evolution of PCOs from a common eukaryotic thiol dioxygenase ancestor occurred early in the plant lineage, while hypoxic induction by ERF-VII factors was only acquired in spermatophytes, and was accompanied by specific alterations in the amino acid sequence of the PCO proteins encoded by these genes.

3.6 | Non-hypoxia-inducible PCOs contribute to control ERF-VII stability

Despite the structural differences highlighted in Figure 1d, A- and B-types PCOs share considerable sequence similarity among taxa, suggesting that their molecular function might be retained throughout evolution. B-type AtPCO1 and AtPCO2 have been shown to promote proteasomal degradation of ERF-VII proteins via the N-degron pathway in vivo and in vitro (Weits et al., 2014;

White et al., 2017). We proceeded to analyze whether A-type AtPCO4 and AtPCO5 are also involved in the regulation of anaerobic responses, by controlling the stability, and thus activity, of proteins with a Cys N-degron in an oxygen dependent manner. First, we tested the subcellular localisation of PCO3, PCO4 and PCO5 fusions to an N-terminal GFP. For comparison, we also repeated the subcellular imaging of GFP-PCO1 and GFP-PCO2 (Weits et al., 2014). A-type PCO3, PCO4 and PCO5 showed nuclear and cytosolic localisation, while B-type PCO1 and PCO2 showed a more predominant signal in the nuclei (Figure 5a; Weits et al., 2014), matching the presence of a region rich in positively charged residues typical of nuclear localisation sequences in PCO1 and PCO2 (Table S8). This result confirmed the potential of A-type PCOs to act on nuclear-localised transcriptional regulators.

Next, we tested the ability of PCO3, PCO4 and PCO5 to restrict ERF-VII activity in vivo by transient expression in mesophyll protoplasts, as was previously shown for B-type PCOs (Weits et al.,

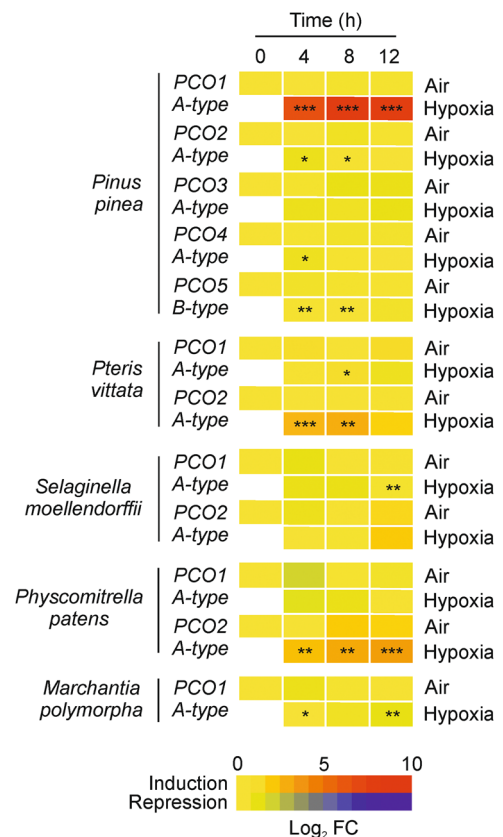


FIGURE 4 Expression analysis of PCOs in response to hypoxia in different plant species that represent subsequent steps in the evolution of land plants. mRNA was extracted from samples treated for 0, 4, 8 and 12 h of dark hypoxia (1% O₂ vol/vol) and the expression of PCOs was compared to that of plants kept under normoxic conditions in the dark ('Air'). Asterisks indicate statistically significant difference from the respective aerated samples after *t* test (*, 0.01 < *p* < 0.05, **, 0.001 < *p* < 0.05, ***, *p* < 0.001; *n* = 4). Unique identifiers for each PCO sequence are provided in Table S3. Numeric expression values are shown in Table S7. mRNA, messenger RNA [Color figure can be viewed at wileyonlinelibrary.com]

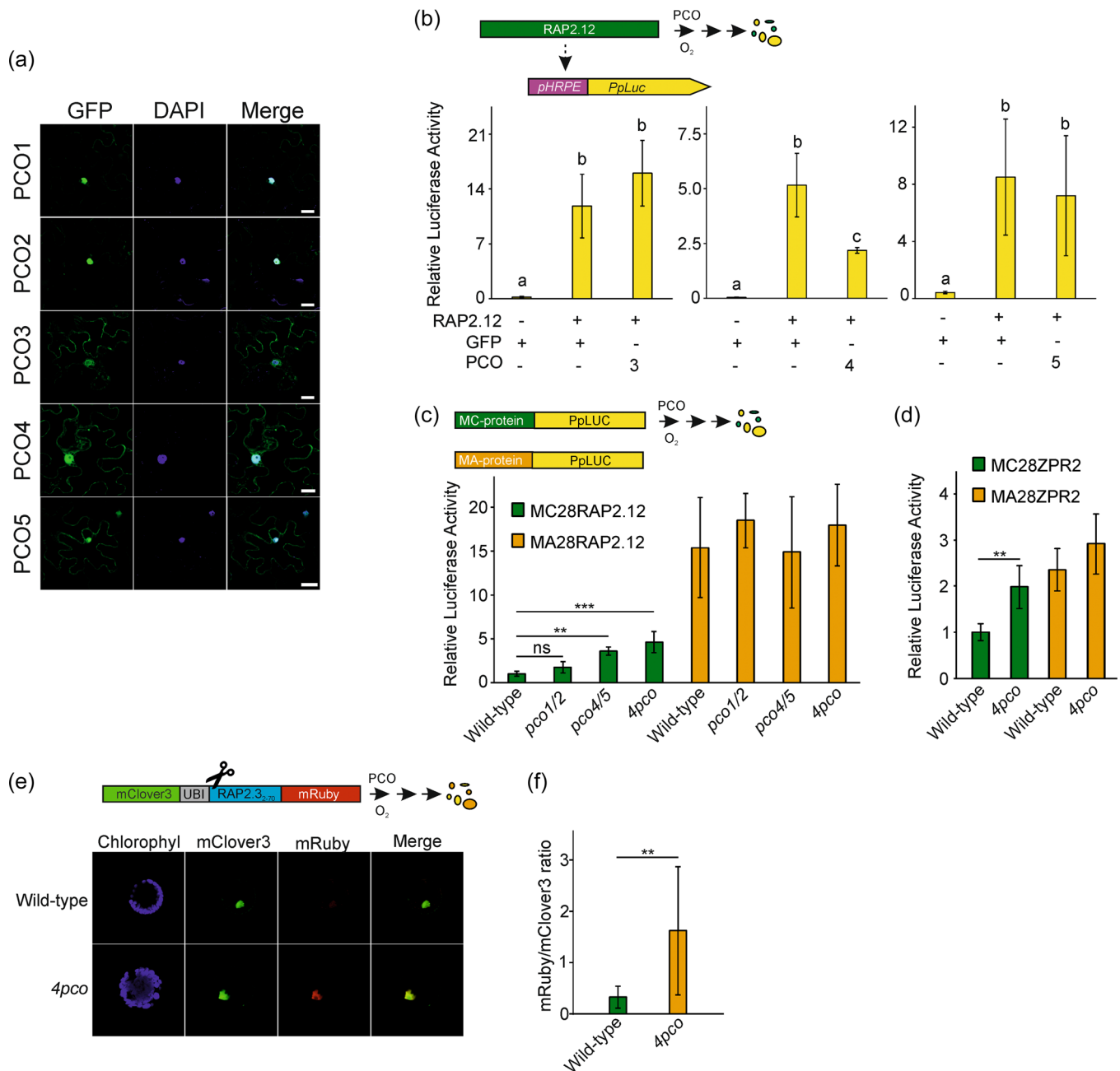


FIGURE 5 Role of A-type PCOs in controlling the activity of Cys-degron proteins. (a) Subcellular localisation of PCO proteins harbouring an N-terminally fused eGFP. Scale bars, 10 μ m. (b) Effect of *PCO4* and *PCO5* expression on transactivation imposed by RAP2.12 in *Arabidopsis thaliana* mesophyll protoplasts. RAP2.12 activity was evaluated on a synthetic promoter harbouring a five time repeat of the hypoxia responsive promoter element (HRPE) fused to a minimal 35S CaMV promoter driving expression of a firefly luciferase (*Photinus pyralis*). A 35S:GFP vector was used as control. Relative luciferase activity (PpLuc/RLuc) were further normalised to GFP-only samples. Data are presented as mean \pm SD ($n = 5$). Letters indicate statistically significant difference ($p < 0.05$, one-way ANOVA, Holm-Sidak post hoc test). The experiment was repeated twice obtaining similar results. (c, d) N-degron reporter activity in plant genotypes with different PCO activity. Protoplasts of wild-type, double *pco1/2* and *pco4/5* mutants and quadruple *4pco* mutants were transiently transformed to express reporter [RAP2.12₁₋₂₈-FLuc in (c) and ZPR2-FLuc in (d)] and normaliser luciferases (35S:RLuc). N-degron substrate reporters are shown in green, while stable reporters are shown in orange. Data are presented as mean \pm SD ($n = 5$, the experiment was repeated twice). Asterisk indicate statistically significant difference [one-way ANOVA followed by Holm-Sidak post hoc test in (d), two-tailed *t* test in (e)]. (e) Design and confocal imaging of a fluorescent dual RAP2.3 reporter in wild-type and *4pco* protoplasts. Ubiquitin (UBI) mediated cleavage exposes the N-terminal 2–70 aa of RAP2.3, which is fused to a red mRuby reporter. In the presence of PCO, RAP2.3₂₋₇₀-mRuby is degraded. A co-translational green mClover3 fluorophore acts as normalisation control. (f) Quantification of fluorescence intensity ratios of mRuby, fused to RAP2.3₂₋₇₀, and mClover3, in wild-type and *4pco* mutants. ANOVA, analysis of variance [Color figure can be viewed at wileyonlinelibrary.com]

2014). To this end, we used the synthetic ERF-VII responsive promoter pHRPE (Kerpen et al., 2019). This was inserted in a reporter vector that bears two luciferase genes, a firefly (*Photinus pyralis*) luciferase under control of the HRPE promoter and a sea pansy (*Renilla reniformis*) luciferase driven by a 35S CaMV promoter, which was used for normalisation purposes. Arabidopsis mesophyll protoplasts were cotransfected with the HRPE reporter, a construct designed to express the ERF-VII transcription factor RAP2.12 and either a vector bearing a PCO gene under control of the 35S promoter, or a GFP sequence as negative control. In this transient assay, PCO4 was able to repress RAP2.12 activity on the HRPE promoter, while PCO3 and PCO5 showed no statistically significant effect (Figure 5b).

We also examined the effect of PCO on ERF-VII stability by using a chimeric reporter protein consisting of the N-terminal 28 aa of RAP2.12 fused to firefly luciferase. To this purpose, we selected Arabidopsis lines bearing a T-DNA within the transcribed sequence of PCO4 and PCO5. We first identified homozygous *pco4* and *pco5* single mutants and subsequently crossed them to generate a double *pco4/5* knock-out mutant (Figure S5). For comparison, a previously identified *pco1/2* mutant was also included in the analysis. The activity of the chimeric reporter in protoplasts was enhanced in both *pco1/2* and *pco4/5* double mutants, and we observed an even stronger RAP2.12₁₋₂₈-PpLUC signal when this reporter was expressed in a *4pco* background where both A-type and B-type PCOs are knocked-out (Figure 5c). This observation indicates that both PCO clades act redundantly to regulate ERF-VII proteolysis. We also observed enhanced stability of a full-length LITTLE ZIPPER 2 (ZPR2)-firefly luciferase fusion in the *4pco* mutant, providing evidence that ZPR2 is also a PCO substrate in vivo (Figure 5d). The signal of MA-initiating versions of both chimeric reporters was comparable between the wild-type and all *pco* knock-out genotypes (Figure 5c,d). This confirmed that proteolysis initiated by PCOs requires an N-terminally exposed cysteine, while the data also indicate that additional regulation may occur at the N-terminally exposed cysteine of the ERF-VII substrate (Figure 5c), possibly via the remaining PCO3 enzyme. Complementary to these approaches, we engineered a ratiometric fluorescence-based reporter for RAP2.3 stability (Figure 5e). In this design, a green emitting mClover3 fluorophore is linked via a ubiquitin monomer to a fusion protein, consisting of the N-terminus of RAP2.3 and a red mRuby fluorescent protein (RAP2.3₂₋₇₀-mRuby, File S1). The ubiquitin monomer confers co-translational cleavage, exposing RAP2.3₂₋₇₀-mRuby to regulation via the N-degron pathway. Expression of this reporter in wild-type protoplasts led to predominantly green fluorescence, while *4pco* mutants showed both mClover3 and mRuby signal, confirming that PCOs are required for proteolysis of RAP2.3 (Figure 5e,f). Taken together, these observations support the hypothesis that A-type PCOs also possess the ability to oxidise N-terminal exposed cysteine and, in angiosperms, both clades act to restrict the anaerobic response by promoting proteolysis of substrates of the N-degron pathway.

3.7 | In Arabidopsis, A-type PCOs play a role to repress the hypoxic response under aerobic conditions

Previously, we showed that PCO1 and PCO2 repress the hypoxic response under aerobic conditions (Weits et al., 2014). Since also PCO4 and PCO5 are able to promote ERF-VII degradation, their inactivation would be expected to lead to an induction of the hypoxic response. We, therefore, aimed at discerning the contribution of each PCO clade on the regulation of the anaerobic response, by analyzing the expression of seven genes that belong to the core anaerobic response (Mustrup et al., 2009) in the *pco1*, *pco2*, *pco3* (Figure S5), *pco4*, *pco5*, *pco1/2*, *pco4/5* and *4pco* mutants and compared their expression to that of wild type plants. The selected genes included those involved in fermentation and metabolism (*Alcohol Dehydrogenase ADH*, *Pyruvate Decarboxylase PDC1*, *Sucrose Synthase SUS1* and *SUS4* (Santaniello et al., 2014), *PHYTOGLOBIN1 PGB1* (Hartman et al., 2019) and signalling (*Hypoxia Responsive Attenuator 1 HRA1* [Giuntoli et al., 2014] and *LOB Domain transcription factor 41 LBD41*). In adult 4-week-old plants and 10-day-old seedlings we could observe only minor effects on the expression of these genes in the *pco1/2* mutants and slightly more evident upregulation in *pco4/5* (Figure 6a and Table S9). Instead, the *4pco* mutant showed a significant increase in the expression of the anaerobic genes when compared to the wild-type, showing that both PCO clades act redundantly under aerobic conditions at this developmental stages (Figure 6a). In 5-day-old seedlings, the effect of *pco4/5* on hypoxia-inducible transcript accumulation under aerobic conditions was more marked, albeit not as strong as in the *4pco* background (Figure 6a and Table S9). These observations show that both PCO groups are involved in the repression of anaerobic responses. Moreover, they confirm the existence of age-dependent effects on the extent of the regulation imposed by the Cys-N degron pathway on the anaerobic genes, as reported before (Giuntoli et al., 2017). At the three stages evaluated, the *pco4/5* mutant showed stronger differences from the wild type than *pco1/2* (Figure 6a), indicating a prominent role for A-type enzymes in repressing the anaerobic response under aerobic conditions, as also suggested by Figure 5c. When plant responses to short-term acute hypoxia were examined (Figure S6 and Table S10), we found A- and B-types PCOs to be functionally redundant under stress conditions as well. Marker gene expression was not overall different from the wild type in either double mutant, with the exception of *PGB1* that displayed stronger induction in *pco4/5*; this mutant also showed a tendency to induce hypoxic-responses faster in the early phase of the stress (1 h hypoxia), but this was non-significant for most hypoxia-inducible genes. Two hour-long reoxygenation was associated with extensive albeit not complete anaerobic mRNA downregulation (Figure S6 and Table S10), in which A- and B-type PCOs took part redundantly again.

Since the expression of hyper-stable versions of ERF-VII and ZPR2 proteins caused altered plant phenotypes (Giuntoli et al., 2017; Weits et al., 2020), we also characterised the consequences of PCO

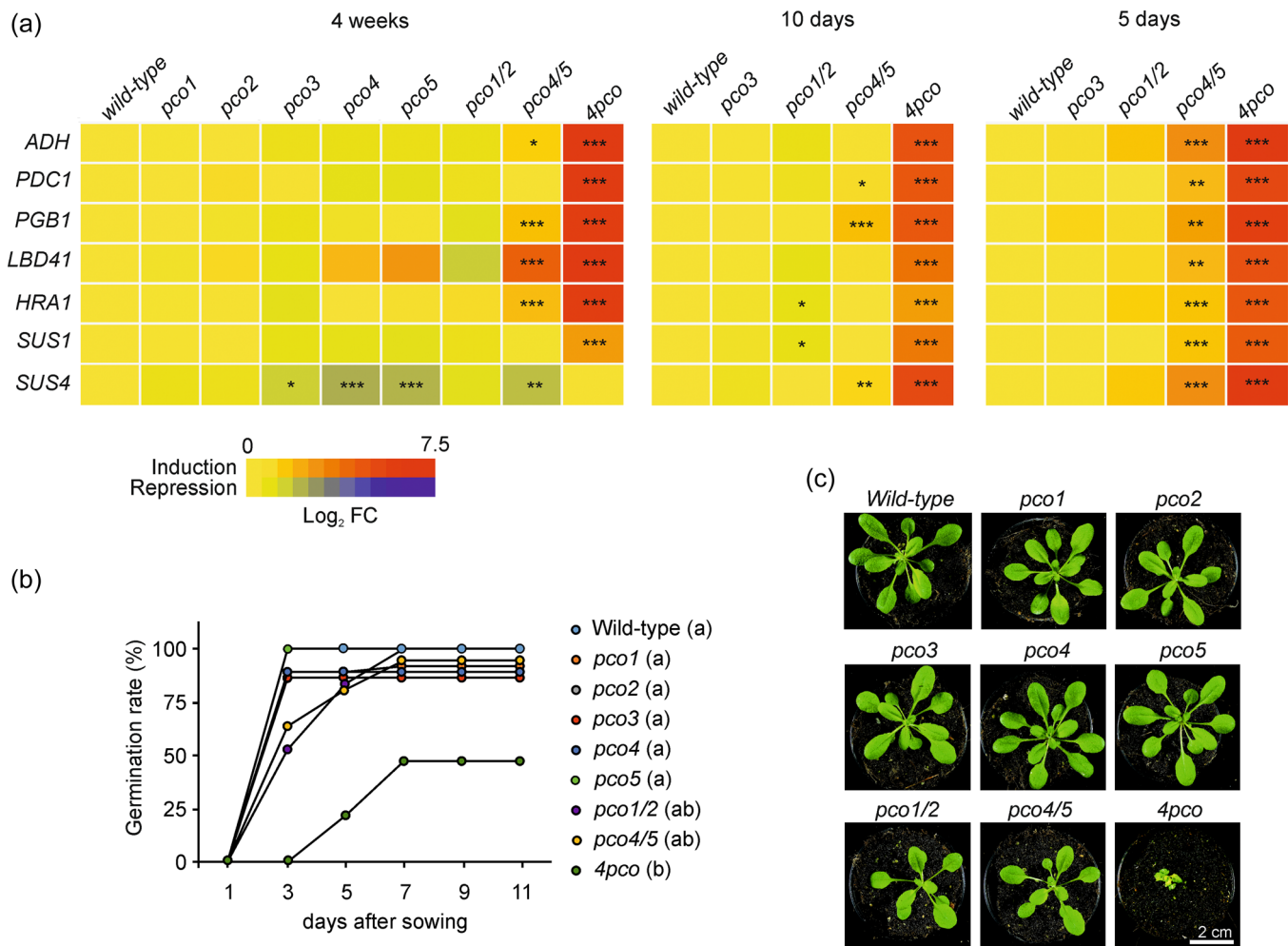


FIGURE 6 Effect of PCO knock out mutants on plant growth and the molecular response to anaerobiosis. (a) Heat map depiction of the transcript levels in full rosettes of 7 genes belonging to the core set of the anaerobic response in single (*pco1*, *pco2*, *pco3*, *pco4* and *pco5*), double (*pco1/2* and *pco4/5*) and quadruple (*4pco*) mutants grown for 4 weeks on soil, 10 days on agarized medium, or 5 days on liquid MS medium under normoxic conditions. Numeric expression values are shown in Table S9. Asterisks indicate statistically significant difference from the wild-type control after 1-way ANOVA and Tukey's post hoc test (*, $0.01 < p < 0.05$, **, $0.001 < p < 0.05$, ***, $p < 0.001$; $n = 5$). (b) Germination percentage of wild-type and *pco* mutant seeds grown in horizontal MS-agar plates. Letters close to the genotype legend indicate grouping according to statistically significant differences, as assessed by Kaplan–Meier survival analysis (log-rank) followed by Holm–Sidak post hoc test. (c) Phenotype of wild-type and *pco* mutants grown in soil for 4 weeks. Scale bar, 2 cm. ANOVA, analysis of variance [Color figure can be viewed at wileyonlinelibrary.com]

inactivation on development and growth. When grown in vertical plates, the high-order *pco* mutants exhibited delayed germination, although this reduction was significant only for the *4pco* genotype, while the single mutants could not be distinguished from the wild type (Figure 6b). Moreover, when grown on soil, *4pco* mutant adult plants developed wrinkled, pale leaves characterised by extensive serration (Figure 6c), as previously described (Masson et al., 2019), while the single and double mutants remained undistinguishable from the wild type. Altogether, the gene expression and phenotypic analyses support a high degree of redundancy among PCO isoforms in controlling the anaerobic response in plants and preventing the developmental consequences of its activation under aerobic conditions.

3.8 | Constitutive induction of anaerobic genes in *pco4/5* mutants affects anaerobic survival

Constitutive activation of the anaerobic response has been shown to have a negative effect on the overall ability of plants to endure actual oxygen deficiency, depending on the experimental conditions employed (Gibbs et al., 2011; Licusi et al., 2011; Riber et al., 2015). Keeping this in mind, we tested the relevance of PCO4 and PCO5 in tolerance to temporary oxygen deficiency. We did not include the quadruple *4pco* mutant in this survey, since its pleiotropic phenotype made it extremely difficult to obtain a sufficient number of homogenous plants to be treated. Its altered normoxic growth also resulted in a remarkably reduced fresh and dry weight, which

hindered proper fitness scoring (Masson et al., 2019; Figure 6c and Figure S7). Thus, we first compared the anoxic survival rate of single *pco4* and *pco5* and double *pco4/5* mutants with that of the wild type when 7-day-old seedlings were grown on a sugar-supplemented medium. In this condition, the double mutant exhibited a significant improvement in anoxic tolerance (Figure 7a,b), possibly due to a primed state of acclimation to anaerobic conditions in the presence of sufficient supply of carbon for glycolysis and fermentation. Indeed, in a separate test conducted with exogenously supplemented sucrose, the *pco4/5* mutant exhibited high fermentative potential under aerobic and hypoxic conditions. In particular, it produced in air

as much ethanol as the wild type after 12 h of hypoxia (Figure 7c). On the other hand, we observed the opposite trend when we exposed soil-grown 4-week-old plants to flooding, as a mean to impose oxygen deprivation: the double *pco4/5* mutant was significantly reduced in terms of biomass production after a 4-day submergence in the darkness (Figure 7d-f). We interpreted this result as a negative effect of enhanced fermentation when plants experience hypoxia in conditions of severe carbon limitation. Surprisingly, the *pco1/2* mutant did not display any growth penalty at the recovery phase, nor did a triple *pco1/2/4* mutant (*3pco*) (Figure 7e,f), suggesting that the presence of one functional type-A PCO gene is crucial and

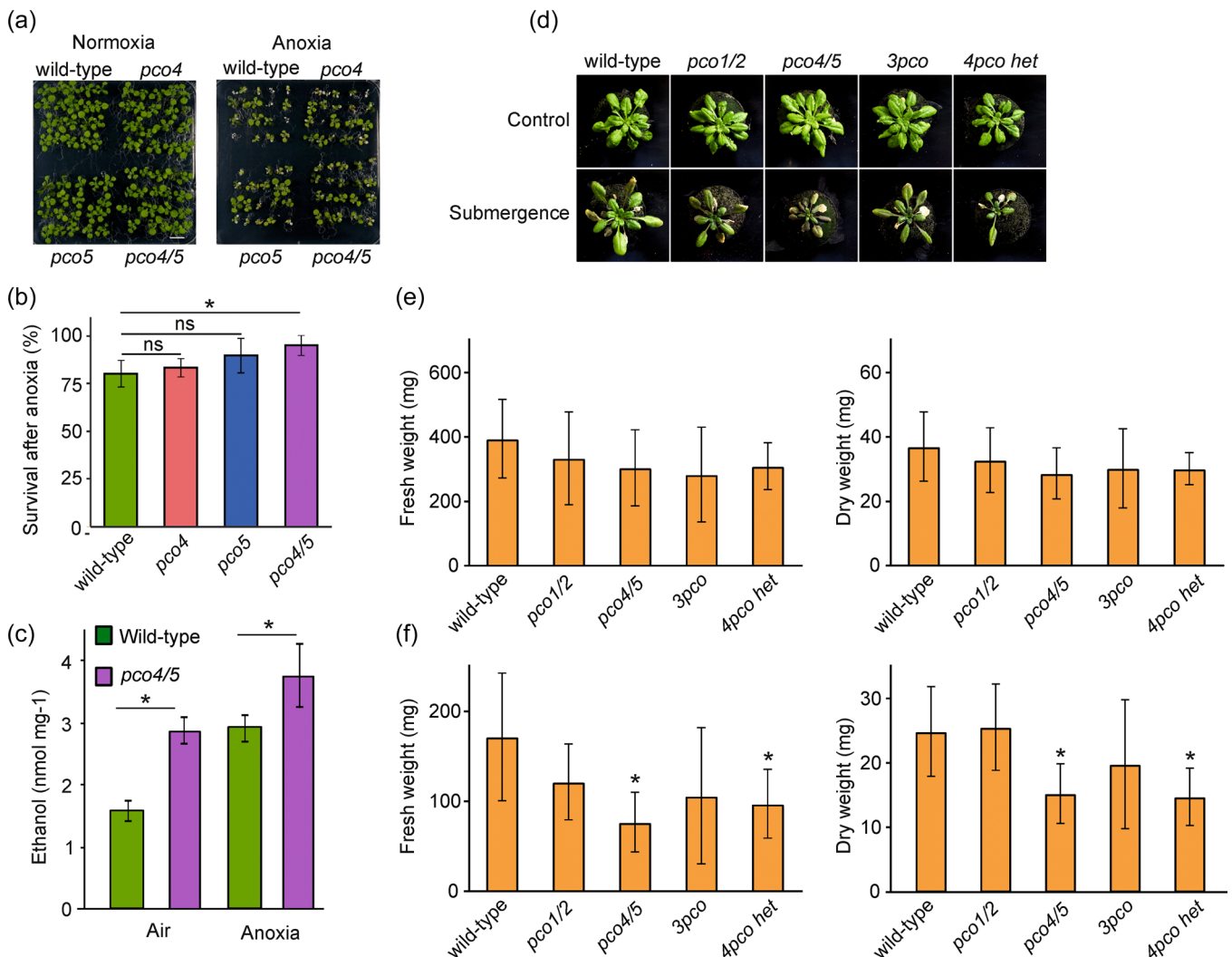


FIGURE 7 Contribution of PCO genes to the tolerance of Arabidopsis plants to low oxygen conditions. (a) Phenotypes of in vitro-grown wild-type, *pco4*, *pco5* and *pco4/5* plants (horizontally grown) 7 days after exposure to 9 h of normoxia or anoxia (<0.01% O₂ vol/vol). Scale bar 1 cm. (b) Percentage of wild-type, *pco4*, *pco5* and *pco4/5* plants surviving 9 h of anoxia in the dark, following a 7-day recovery period. (c) Ethanol production in tissues of wild-type and the double *pco4/5* mutant. 1-week-old plants (horizontally grown) were transferred to sterile media containing 2% (wt/vol) sucrose, 12 h before being incubated for 12 h with anoxia (<0.01% O₂ vol/vol) or normoxia. The plots are built on the basis of five replicates. (d) Phenotypes of 4-week-old soil-grown wild-type, *pco1/2*, *pco4/5*, *pco1pco2pco4* (*3pco*) and *4pco* with *pco5* in heterozygosity plants recovering from 6 days of complete submergence in the dark. (e, f) Biomass (dry and fresh weight) of wild-type, *pco1/2*, *pco4/5*, *pco1pco2pco4* (*3pco*) and *4pco* with *pco5* in heterozygosity plants following 4 d of recovery from dark (e) and dark submergence (f) (n = 8). Asterisks indicate statistically significant difference from wild type (p < 0.05, one-way ANOVA). ANOVA, analysis of variance [Color figure can be viewed at wileyonlinelibrary.com]

sufficient to enable *Arabidopsis* to withstand this stress condition. Biomass production was indeed already impaired when a heterozygous *pco5* mutation was added to the triple mutant background (*4pco* het.).

4 | DISCUSSION

In the present study, a phylogenetic analysis of the occurrence of NCO sequences among eukaryotes revealed that these are ubiquitously present in the plant kingdom (Figure 2), as they are in the animal one (Masson et al., 2019). Sequences with high similarity to PCOs were fixed in embryophytes, possibly already to catalyze N-terminal cysteine oxidation, where this family proliferated due to genome duplication events. Among the classes of Cys-starting proteins identified so far in plants as PCO substrates, ERF-VIIs seem to be the earliest to be fixed in vascular plants, while ZPR2 and VRN2 proteins followed, in angiosperms (Figure 2). This suggests a progressive co-adaptation with PCO to accommodate the N-terminal degron to PCO activity. It is tempting to speculate about the requirement for an ERF-VII/PCO circuit when, with vascularisation, plants acquired a level of complexity that entails internal oxygen gradients (Van Dongen & Licausi, 2015). Hypoxia-responsiveness is not a general feature of PCO proteins. All early evolved PCOs identified in our analysis bear the distinctive sequence features of non hypoxia-inducible PCOs, which we defined here as A-type PCOs (Figure 1c,d). Our analysis indicates that, instead, hypoxia-inducible B-type PCOs represent a relatively recent acquisition by spermatophytes, where a second group branched out from the original family (Figure 1c). The innovation of these B-type PCOs is not limited to the protein sequence, where we could identify three main signature motifs that distinguish A- and B-types PCOs (Figure 1d), but also extends to the acquisition of an HRPE DNA element, in the promoter of their respective genes, that confers ERF-VII mediated regulation under hypoxia (Table S3). The conserved co-occurrence of this cis-regulatory feature and structural characteristics is suggestive of an optimisation of anaerobiosis-inducible isoforms to reduced oxygen availability. In this way, B-type PCOs may play a role during fluctuating hypoxia to specifically recognise ERF-VII proteins to ensure efficient and rapid restraint of anaerobic responses such as fermentation, whose excess has been shown to be detrimental for plant survival under submergence (Licausi et al., 2011; Paul et al., 2016). Remarkably, the need of a similar feedback loop has also been reported for mammals. Here, the oxygen sensing enzymes prolyl dehydrogenases (PHDs) control the stability of the α subunit of the hypoxia-inducible factor-1 complex, which, in turn, further upregulates *PHD* expression (Henze & Acker, 2010).

As mentioned above, NCOs seem to be ubiquitously distributed and conserved in the plant and animal kingdom. Fungi, on the other hand, represent a peculiar case: we could only find NCO-like sequences in chytridiomycota, one of the early diverging lineages of this kingdom, but not in other groups (Figure 3a). Not all chytrid species tested possess a PCO-like sequence, suggesting that this gene is not essential

for the biology of these organisms (Figure S4). The fact that chytrids thrive in aquatic habitats, and water is necessary for the movement of chytrid zoospores, support the hypothesis of NCO-like sequences being involved in oxygen sensing in these organism (Kagami et al., 2014). In this perspective, NCO-mediated responses might help to cope with oxygen fluctuations in aquatic environments. Future characterisation of fungal NCOs and their substrates, both in vivo and in vitro, will shed light on these aspects.

The absence of NCO-like sequences in all other groups might indicate that this has been lost early during fungal evolution, except in chytrids, possibly because it affected fitness negatively. However, expression of plant PCO or human ADO in the budding yeast *Saccharomyces cerevisiae* did not impair cell growth, opposing the idea of toxicity of this gene in fungi (Masson et al., 2019; Puerta et al., 2019). Alternatively, horizontal gene transfer might have led to NCO fixation in chytrid genomes. Indeed, several chytrids parasitise animal or plants species. The closest similarity of chytrid NCOs to PCOs rather than animal ADOs would favour the hypothesis of an acquisition from a plant donor (Figure 3b,c). In support of this, chytrid fossils from the Rhynie chert, a Devonian-age lagerstätte, are parasites of rhyniophytes, demonstrating early establishment of plant parasitism (Taylor et al., 1994).

As mentioned above, the A-type PCOs do not exhibit conserved responsiveness to hypoxia at the transcript level. Nevertheless, PCO4 has been confirmed as a potential initiator of the proteolytic N-degron pathway in vitro (White et al., 2017), is sufficient to complement the growth defects of the *4pco* mutant to a wild type phenotype (White et al., 2020) and has been shown to retain the highest catalytic power in RAP2.12 processing (White et al., 2018). Indeed, PCO4 proved to be very effective in repressing RAP2.12 activity in our transient assay, and inhibiting the accumulation of N-degron reporters (Figure 5b-d). The observation that a concomitant knocking-out of *PCO4* and *PCO5* genes induces activation of the anaerobic response in young *Arabidopsis* seedlings (Figure 6a) indicates that their affinity for ERF-VII is sufficient in vivo to control the stability of these TFs under aerobic conditions. On the other hand, at later stages, the remaining PCO enzymes in *Arabidopsis*, or parallel repressive mechanisms, were sufficient to repress ERF-VII activity and thus induction of anaerobic genes (Figure 6a). We reported similar observations for other mutants of the N-degron pathway, whose weight in the further processing of substrates with N-terminal Cys progressively decreases as plants age (Giuntoli et al., 2017). Remarkably, while loss of four out of five PCO enzymes deregulates the anaerobic response, A- and B-types PCOs showed a strong degree of complementation in *Arabidopsis*, except for young seedlings, where A-type have a prominent role. Moreover, *Arabidopsis* does not appear to fully exploit its repertoire of A- and B-types PCOs to tune hypoxic-responses (Figure S6), while this may not hold true for flooding tolerant plant species. The existence of specific functions of PCO clades should therefore be studied in adapted species. It is also interesting to note that all five PCO sequences analyzed so far can enter the nucleus (Figure 5a, Weits et al., 2014), although B-type PCOs appear to accumulate more

strongly to the nucleus and are predicted to contain at least one known nuclear localisation sequence. This suggests that A-type PCOs may be imported into the nucleus by a different mechanism.

Assuming that one of the roles of the PCOs is to restrain the activation of fermentation under aerobic conditions, it is not surprising that their absence negatively affects plant fitness, as seen by a decrease in germination speed and shoot growth in the *4pco* mutant (Figure 6b,c and Figure S7). It is likely that these plants are exposed to a similar metabolic stress as that identified in plants expressing a stabilised version of RAP2.12 (Paul et al., 2016). Additional explanation for the *4pco* phenotype may be found in the constitutive stabilisation of the Cys-degron proteins VRN2 and ZPR2, which are in vitro and in vivo PCO substrates respectively (Gibbs et al., 2018; Figure 5d). VRN2 and ZPR2 regulate different aspects of plant development and accumulate in meristematic niches, tissues that have been characterised as chronically hypoxic (Gibbs et al., 2018; Shukla et al., 2019; Weits et al., 2020). Excessive abundance of these MC proteins in *4pco* mutants may therefore also play a role in causing its peculiar phenotype.

When single or double *pco* mutants, which do now show remarkable morphologic alterations under non-stress conditions, are challenged with oxygen deprivation, their performance strongly depends on the availability of carbon resources to support energy production via glycolysis coupled to fermentation. Indeed, double *pco4/5* mutants showed increased survival rate to anoxic exposure when grown in the presence of exogenous sucrose (Figure 7a,b), whereas they were impaired in biomass maintenance when grown in soil and subjected to prolonged submergence (Figure 7d–f). In the past, contrasting results have been obtained when comparing plants compromised in ERF-VII degradation and subjected to oxygen deprivation (Gibbs et al., 2011; Licausi et al., 2011). Most divergent outcomes have been reported in the case of submergence, which is a compound stress that involves several factors in addition to reduced oxygen availability (Bailey-Serres & Colmer, 2014). An extensive analysis of the possible reasons for this have been carried out by Riber and colleagues (2015), pointing at the importance of humidity in post-submergence conditions and the content and usage of carbon reserves in the plant. Due to the high relevance of this topic for crop breeding and farming practices, most useful and conclusive information on this matter is likely to come from the analysis of plant performance, when grown and challenged with submergence in proper agricultural conditions, namely in open fields.

In conclusion, the study presented here allows for a subdivision of PCOs into two clades based on their amino acid sequence and their transcriptional regulation: those that are induced upon hypoxia (B-type) and those whose expression is unaffected by oxygen limitation (A-type). Both PCO clades are involved in the repression of the anaerobic response under normoxic conditions. Interestingly, A-type PCOs are present ubiquitously, whereas the B-type enzymes have evolved with spermatophytes. In gymnosperms and angiosperms, the hypoxia-inducible clade PCOs may, therefore, have evolved as a mechanism to fine-tune the extent of the anaerobic response to the strength of the hypoxic stress. The Arabidopsis

proteome contains over 200 proteins with a cysteine in amino terminal position. These proteins are all potentially targets of PCOs and their identification may lead to more information on which other processes may be regulated by the oxygen-dependent branch of the N-degron pathway for protein degradation.

ACKNOWLEDGEMENTS

Results have been achieved within the framework of the PRIN2017 project 20173EWRT9 funded by the Italian Ministry of University and Research and the ERC Consolidator Grant project101001320–SynOxyS. Lina Zhou was financially supported by the China Scholarship Council.

ORCID

Beatrice Giuntoli  <http://orcid.org/0000-0003-4968-4071>

Francesco Licausi  <http://orcid.org/0000-0003-4769-441X>

REFERENCES

- Altschul, S.F., Gish, W., Miller, W., Myers, E.W. & Lipman, D.J. (1990) Basic local alignment search tool. *Journal of Molecular Biology*, 215, 403–410.
- Bachmair, A., Finley, D. & Varshavsky, A. (1986) In vivo half-life of a protein is a function of its amino-terminal residue. *Science*, 234, 179–186.
- Bailey, I.L., Boden, M., Buske, F.A., Martin Frith, M., Grant, C.E., Clementi, L. et al. (2009) MEME SUITE: tools for motif discovery and searching—PubMed. *Nucleic Acids Research*, 37, 202–208.
- Bailey-Serres, J. & Colmer, T.D. (2014) Plant tolerance of flooding stress—recent advances. *Plant Cell & Environment*, 37, 2211–2215.
- Chang, Y., Wang, S., Sekimoto, S., Aerts, A.L., Choi, C., Clum, A. et al. (2015) Phylogenomic analyses indicate that early fungi evolved digesting cell walls of algal ancestors of land plants. *Genome Biology and Evolution*, 7, 1590–1601.
- Chung, H.S., Wang, S.B., Venkatraman, V., Murray, C.I. & Van Eyk, J.E. (2013) Cysteine oxidative post-translational modifications: emerging regulation in the cardiovascular system. *Circulation Research*, 112, 382–392.
- Clough, S.J. & Bent, A.F. (1998) Floral dip: a simplified method for agrobacterium-mediated transformation of arabidopsis thaliana. *The Plant Journal*, 16, 735–743.
- Dalle Carbonare, L.D., White, M.D., Shukla, V., Francini, A., Perata, P., Flashman, E. et al. (2019) Zinc excess induces a hypoxia-like response by inhibiting cysteine oxidases in poplar roots. *Plant Physiology*, 180(3), 1614–1628.
- Van Dongen, J.T. & Licausi, F. (2015) Oxygen sensing and signaling. *Annual Review of Plant Biology*, 66, 345–367.
- Edgar, R.C. (2004) MUSCLE: multiple sequence alignment with high accuracy and high throughput. *Nucleic Acids Research*, 32, 1792–1797.
- Gasch, P., Fundinger, M., Müller, J.T., Lee, T., Bailey-Serres, J. & Mustroph, A. (2016) Redundant ERF-VII transcription factors bind to an evolutionarily conserved cis-motif to regulate hypoxia-responsive gene expression in arabidopsis. *The Plant Cell*, 28, 160–180.
- Gibbs, D.J., Lee, S.C., Isa, N.M., Gramuglia, S., Fukao, T., Bassel, G.W. et al. (2011) Homeostatic response to hypoxia is regulated by the N-end rule pathway in plants. *Nature*, 479, 415–418.
- Gibbs, D.J., Md Isa, N., Movahedi, M., Lozano-Juste, J., Mendiando, G.M., Berckhan, S. et al. (2014) Nitric oxide sensing in plants is mediated by proteolytic control of group VII ERF transcription factors. *Molecular Cell*, 53, 369–379.

- Gibbs, D.J., Tedds, H.M., Labandera, A.M., Bailey, M., White, M.D., Hartman, S. et al. (2018) Oxygen-dependent proteolysis regulates the stability of angiosperm polycomb repressive complex 2 subunit VERNALIZATION 2. *Nature Communications*, 9, 5438.
- Giuntoli, B., Lee, S.C., Licausi, F., Kosmacz, M., Oosumi, T., van Dongen, J.T. et al. (2014) A trihelix DNA binding protein counterbalances hypoxia-responsive transcriptional activation in arabidopsis. *PLoS Biology*, 12, e1001950.
- Giuntoli, B., Shukla, V., Maggiorini, F., Giorgi, F.M., Lombardi, L., Perata, P. et al. (2017) Age-dependent regulation of ERF-VII transcription factor activity in *Arabidopsis thaliana*. *Plant, Cell and Environment*, 40, 2333–2346.
- Graciet, E., Mesiti, F. & Wellmer, F. (2010) Structure and evolutionary conservation of the plant N-end rule pathway. *The Plant Journal*, 61, 741–751.
- Graciet, E. & Wellmer, F. (2010) The plant N-end rule pathway: structure and functions. *Trends in Plant Science*, 15, 447–453.
- Grigoriev, I.V., Nikitin, R., Haridasb, S., Kuo, A., Ohmv, R., Otilar, R. et al. (2014) MycoCosm portal: gearing up for 1000 fungal genomes. *Nucleic Acids Research*, 42, 699–704.
- Gunawardana, D.M., Heathcote, K.C. & Flashman, E. (2022) Emerging roles for thiol dioxygenases as oxygen sensors. *FEBS J*, 289, 5426–5439. <https://doi.org/10.1111/febs.16147>
- Hartman, S., Liu, Z., van Veen, H., Vicente, J., Reinen, E., Martopawiro, S. et al. (2019) Ethylene-mediated nitric oxide depletion pre-adapts plants to hypoxia stress. *Nature Communications*, 10, 4020.
- Hellens, R.P., Allan, A.C., Friel, E.N., Bolitho, K., Grafton, K. & Templeton, M.D. et al. (2005) Transient expression vectors for functional genomics, quantification of promoter activity and RNA silencing in plants. *Plant Methods*, 1, 13.
- Henze, A. & Acker, T. (2010) Feedback regulators of hypoxia-inducible factors and their role in cancer biology. *Cell Cycle*, 14, 2749–2763.
- Holdsworth, M.J. & Gibbs, D.J. (2020) Comparative biology of oxygen sensing in plants and animals. *Current Biology*, 30, R362–R369.
- Hu, R.G., Sheng, J., Qi, X., Xu, Z., Takahashi, T.T. & Varshavsky, A. (2005) The N-end rule pathway as a nitric oxide sensor controlling the levels of multiple regulators. *Nature*, 437, 981–986.
- Iacopino, S., Jurinovich, S., Cupellini, L., Piccinini, L., Cardarelli, F., Perata, P. et al. (2019) A synthetic oxygen sensor for plants based on animal hypoxia signaling. *Plant Physiology*, 179, 986–1000.
- Iacopino, S. & Licausi, F. (2020) The contribution of plant dioxygenases to hypoxia signaling. *Frontiers of Plant Science*, 11, 1008.
- Jones, D.T., Taylor, W.R. & Thornton, J.M. (1992) The rapid generation of mutation data matrices from protein sequences - PubMed. *Computer Applications in the Biosciences*, 8, 275–282.
- Kagami, M., Miki, T. & Takimoto, G. (2014) Mycoloop: chytrids in aquatic food webs. *Frontiers in Microbiology*, 5, 166.
- Karimi, M., Inzé, D. & Depicker, A. (2002) GATEWAY® vectors for agrobacterium-mediated plant transformation. *Trends in Plant Science*, 7, 193–195.
- Kerpen, L., Niccolini, L., Licausi, F., van Dongen, J.T. & Weits, D.A. (2019) Hypoxic conditions in crown galls induce plant anaerobic responses that support tumor proliferation. *Frontiers of Plant Science*, 10, 56.
- Kosmacz, M., Parlanti, S., Schwarzlaender, M., Kragler, F., Licausi, F. & Van Dongen, J.T. (2015) The stability and nuclear localization of the transcription factor RAP2.12 are dynamically regulated by oxygen concentration. *Plant, Cell & Environment*, 38, 1094–1103.
- Kumar, S., Stecher, G., Li, M., Knyaz, C. & Tamura, K. (2018) MEGA X: molecular evolutionary genetics analysis across computing platforms. *Molecular Biology and Evolution*, 35, 1547–1549.
- Labandera, A.M., Tedds, H.M., Bailey, M., Sprigg, C., Etherington, R.D., Akintewe, O. et al. (2020) The PRT6 N-degron pathway restricts VERNALIZATION 2 to endogenous hypoxic niches to modulate plant development. *New Phytologist*, 229, 126–139. Available at <https://doi.org/10.1111/nph.16477>
- Licausi, F., van Dongen, J.T., Giuntoli, B., Novi, G., Santaniello, A., Geigenberger, P. et al. (2010) HRE1 and HRE2, two hypoxia-inducible ethylene response factors, affect anaerobic responses in *Arabidopsis thaliana*. *The Plant Journal*, 62, 302–315.
- Licausi, F., Kosmacz, M., Weits, D.A., Giuntoli, B., Giorgi, F.M., Voesenek, L.A.C.J. et al. (2011) Oxygen sensing in plants is mediated by an N-end rule pathway for protein destabilization. *Nature*, 479, 419–422.
- Liu, Y.Y., Yang, K.Z., Wei, X.X. & Wang, X.Q. (2016) Revisiting the phosphatidylethanolamine-binding protein (PEBP) gene family reveals cryptic FLOWERING LOCUS T gene homologs in gymnosperms and sheds new light on functional evolution. *New Phytologist*, 212, 730–744.
- Masson, N., Keeley, T.P., Giuntoli, B., White, M.D., Puerta, M.L., Perata, P. et al. (2019) Conserved N-terminal cysteine dioxygenases transduce responses to hypoxia in animals and plants. *Science*, 365, 65–69.
- McCoy, J.G., Bailey, L.J., Bitto, E., Bingman, C.A., Aceti, D.J., Fox, B.G. et al. (2006) Structure and mechanism of mouse cysteine dioxygenase. *Proceedings of the National Academy of Sciences of the United States of America*, 103, 3084–3089.
- Mustroph, A., Zanetti, M.E., Jang, C.J.H., Holtan, H.E., Repetti, P.P., Galbraith, D.W. et al. (2009) Profiling translomes of discrete cell populations resolves altered cellular priorities during hypoxia in *Arabidopsis*. *Proceedings of the National Academy of Sciences*, 106, 18843–18848.
- Panicucci, G., Iacopino, S., De Meo, E., Perata, P. & Weits, D.A. (2020) An improved HRPE-based transcriptional output reporter to detect hypoxia and anoxia in plant tissue. *Biosensors*, 10(2020), 197.
- Paul, M.V., Iyer, S., Amerhauser, C., Lehmann, M., van Dongen, J.T. & Geigenberger, P. (2016) RAP2.12 oxygen sensing regulates plant metabolism and performance under both normoxia and hypoxia. *Plant Physiology*, 172, 141–153.
- Puerta, M.L., Shukla, V., Dalle Carbonare, L., Weits, D.A., Perata, P., Licausi, F. et al. (2019) A ratiometric sensor based on plant N-terminal degrons able to report oxygen dynamics in *Saccharomyces cerevisiae*. *JMB*, 431, 2810–2820.
- Reddie, K.G. & Carroll, K.S. (2008) Expanding the functional diversity of proteins through cysteine oxidation. *Current Opinion in Chemical Biology*, 12, 746–754.
- Reski, R. & Abel, W.O. (1985) Induction of budding on chloronemata and caulonemata of the moss, *Physcomitrella patens*, using isopentenyladenine. *Planta*, 165, 354–358.
- Riber, W., Müller, J.T., Visser, E.J., Sasidharan, R., Voesenek, L.A. & Mustroph, A. (2015) The greening after extended Darkness1 is an N-End rule pathway mutant with high tolerance to submergence and starvation. *Plant Physiology*, 167, 1616–1629.
- Santaniello, A., Loreti, E., Gonzali, S., Novi, G. & Perata, P. (2014) A reassessment of the role of sucrose synthase in the hypoxic sucrose-ethanol transition in arabidopsis. *Plant Cell & Environment*, 37, 2294–2302.
- Shukla, V., Lombardi, L., Iacopino, S., Pencik, A., Novak, O., Perata, P. et al. (2019) Endogenous hypoxia in lateral root primordia controls root architecture by antagonizing auxin signaling in arabidopsis. *Molecular Plant*, 12, 538–551.
- Tasaki, T., Sriram, S.M., Park, K.S. & Kwon, Y.T. (2012) The N-end rule pathway. *Annual Review of Biochemistry*, 81, 261–289.
- Taylor, T.N., Remy, W. & Hass, H. (1994) Allomyces in the Devonian. *Nature*, 367, 601.
- Taylor-Kearney, L.J., Madden, S., Wilson, J., Myers, W.K., Gunawardana, D.M., Pires, E. et al. (2022) Plant cysteine oxidase oxygen-sensing function is conserved in early land plants and algae. *ACS Bio & Med Chem Au*. Available at <https://doi.org/10.1021/acsbiochemau.2c00032>

- Weits, D.A., van Dongen, J.T. & Licausi, F. (2020) Molecular oxygen as a signaling component in plant development. *New Phytologist*, 229, 24–35. Available at <https://doi.org/10.1111/nph.16424>
- Weits, D.A., Giuntoli, B., Kosmacz, M., Parlanti, S., Hubberten, H.M. & Riegler, H. et al. (2014) Plant cysteine oxidases control the oxygen-dependent branch of the N-end-rule pathway. *Nature Communications*, 5, 3425.
- Weits, D.A., Kunkowska, A.B., Kamps, N.C.W., Portz, K.M.S., Packbier, N.K., Nemeč Venzá, Z. et al. (2019) An apical hypoxic niche sets the pace of shoot meristem activity. *Nature*, 569, 714–717.
- White, M.D., Dalle Carbonare, L., Lavilla Puerta, M., Iacopino, S., Edwards, M., Dunne, K. et al. (2020) Structures of *Arabidopsis thaliana* oxygen-sensing plant cysteine oxidases 4 and 5 enable targeted manipulation of their activity. *Proceedings of the National Academy of Sciences*, 117(37), 23140–23147.
- White, M.D., Kamps, J.J.A.G., East, S., Taylor-Kearney, L.J. & Flashman, E. (2018) The plant cysteine oxidases from *Arabidopsis thaliana* are kinetically tailored to act as oxygen sensors. *Journal of Biocommunication*, 293, 11786–11795.
- White, M.D., Klecker, M., Hopkinson, R.J., Weits, D.A., Mueller, C., Naumann, C. et al. (2017) Plant cysteine oxidases are dioxygenases that directly enable arginyl transferase-catalysed arginylation of N-end rule targets. *Nature Communications*, 8, 14690.

SUPPORTING INFORMATION

Additional supporting information can be found online in the Supporting Information section at the end of this article.

How to cite this article: Weits, D.A., Zhou, L., Giuntoli, B., Carbonare, L.D., Iacopino, S., Piccinini, L., et al. (2023) Acquisition of hypoxia inducibility by oxygen sensing N-terminal cysteine oxidase in spermatophytes. *Plant, Cell & Environment*, 46, 322–338.
<https://doi.org/10.1111/pce.14440>